A multi-tracer approach to constraining artesian groundwater discharge into an alluvial aquifer

Authors: Charlotte P. Iverach[1,2,3], Dioni I. Cendón[1,2,3], Karina T. Meredith[3], Klaus M. Wilcken[3], Stuart I. Hankin[3], Martin S. Andersen[1,4], Bryce F.J. Kelly[1,2,*]

[1]Connected Waters Initiative Research Centre, UNSW Sydney, NSW, 2052, Australia

[2]School of Biological, Earth and Environmental Sciences, UNSW Sydney, NSW, 2052, Australia.

[3]Australian Nuclear Science and Technology Organisation, New Illawarra Rd, Lucas Heights, NSW, 2234, Australia.

[4]School of Civil and Environmental Engineering, UNSW Sydney, NSW, 2052, Australia.

*Corresponding author: bryce.kelly@unsw.edu.au

Understanding pathways of recharge to alluvial aquifers is important for maintaining sustainable access to groundwater resources. Water balance modelling is often used to proportion recharge components and guide sustainable groundwater allocations. However, it is not common practice to use hydrochemical evidence to inform and constrain these models. Here we compare geochemical versus water balance model estimates of artesian discharge into an alluvial aquifer, and demonstrate why multi-tracer geochemical analyses should be used as a critical component of water budget assessments. We selected a site in Australia where the Great Artesian Basin (GAB), the largest artesian basin in the world, discharges into the Lower Namoi Alluvium (LNA), an extensively modelled aquifer, to convey the utility of our approach. Water stable isotopes ($\delta^{18}O$ and $\delta^{2}H$) and the concentrations of Na^{+} and HCO_3^{-} suggest a continuum of mixing in the alluvial aquifer between the GAB (artesian component) and surface recharge, whilst isotopic tracers (^{3}H, ^{14}C and ^{36}Cl) indicate that the alluvial groundwater is a mixture of groundwaters with residence times of < 70 years using ^{3}H and ~ 900 ka using ^{36}Cl methods. In addition, Cl^{-} concentrations provide a means to calculate a percentage estimate of the artesian contribution to the alluvial groundwater. In some locations, an artesian contribution of up to 70% is evident from the geochemical analyses, a finding that contrasts previous water balance modelling estimates of 22%. Our results show that hydrochemical investigations need to be undertaken as part of developing the conceptual framework of a catchment water balance model, as they can improve our understanding of recharge pathways and better constrain artesian discharge to an alluvial aquifer.

1 Introduction

Recharge to alluvial aquifers can occur via infiltration from the land surface and/or discharge into the alluvium from surrounding geological formations and artesian groundwater resources (Costelloe et al. 2012; Schilling et al. 2016; Rawling & Newton 2016; Salameh et al. 2017). Insufficient spatial and temporal data resolution, as well as heterogeneity in hydrogeological properties can result in considerable uncertainty when allocating recharge to each source (Anderson & Woessner 1992; Beven 2009; Gardner et al. 2012). Additional uncertainties when allocating recharge to each source include change in the magnitude of groundwater gradients and directions over time due to ongoing groundwater abstraction (for irrigation, stock and domestic water supplies), and the impact that this and flood frequency may have on the extent of artesian discharge and groundwater mixing. These complexities make it challenging to accurately proportion contributions from various sources to an alluvial aquifer and to guide water allocations.

Water balance modelling of alluvial aquifers is commonly used to quantify and proportion recharge inputs from river leakage, floodwaters, areal (diffuse recharge) and artesian sources (Anderson & Woessner 1992; Middlemis et al. 2000; Zhang et al. 2002; Dawes et al. 2004; Barnett et al. 2012; Giambastiani et al. 2012; Hocking & Kelly 2016). Historically, hydrochemical analyses are not often used to constrain catchment scale water balance modelling (Reilly and Harbaugh 2004; Barnett et al. 2012), despite Scanlon et al. (2004) highlighting the need to use multiple techniques (including hydrochemical insights) to increase the reliability of recharge estimates. Geochemical data can improve our understanding of recharge processes because of the potential to trace pathways of groundwater movement and water-rock interactions, whilst also providing insights on the impacts of past groundwater extractions (Martinez et al. 2017). Therefore, the integration of geochemical evidence to constrain aquifer water balance models provides a more rigorous

approach for estimating and proportioning sources of recharge to groundwater resources (Raiber et al. 2015; Currell et al. 2017).

Radioactive isotopic tracers that provide insights into groundwater residence times can constrain mechanisms of recharge and detect groundwater mixing. Isotopes of dissolved species can be useful for elucidating groundwater mixing provided the different sources of groundwater have distinctly different and consistent isotopic signatures. However, each tracer has a different half-life and undergoes processes specific to it that can often affect interpretations. Thus, these tracers can provide process insights but only for a given window of time. Therefore, multiple tracers are needed to cover the time scales relevant for the large range required for groundwater residence times. Tritium (^{3}H) is an excellent indicator of modern recharge inputs in shallow groundwater (Robertson et al. 1989; Chen et al. 2006; Duvert et al. 2016), and provides valuable information on processes active in the past ~ 70 years. Carbon-14 (^{14}C) is used to understand processes active from modern to ~ 30 ka (Clark & Fritz 1997; Cartwright et al. 2010; Cendón et al. 2014) and chlorine-36 (^{36}Cl), whilst applicable in modern groundwater (Tosaki et al. 2007), is usually reserved for the identification of much older groundwater (100 ka to 1 Ma). One of the challenges of using ^{36}Cl is that, in certain cases, nucleogenic production of ^{36}Cl can be significant and/or varying Cl concentrations can complicate groundwater residence time interpretations. However, in regions with low and fairly consistent Cl concentrations (such as in our study area), ^{36}Cl values can provide solid indications of old groundwater residence times (Mahara et al. 2007).

These isotopes can also be used for tracer mixing calculations independent of residence time estimations (Bentley et al. 1986; Andrews & Fontes 1993; Love et al. 2000; Moya et al. 2016). Therefore, the combination of ^{3}H, ^{14}C, and ^{36}Cl dating techniques can provide hydrochemical process insights that cannot be captured by using only one isotope.

Identification of recharge and discharge pathways, particularly from underlying artesian contributions, can be better constrained by combining traditional geochemical data with multiple dating techniques and other hydrologic analyses (Amiri et al. 2016; Rawling & Newton 2016; Schilling et al. 2016). Here, we present for the first time a multi-tracer approach to constraining artesian discharge from the Great Artesian Basin (GAB) into the Lower Namoi Alluvium (LNA), north-west New South Wales (NSW), Australia (Figure 1). We use water stable isotopes and major ion data to assess the major recharge pathways and occurrences of groundwater mixing in the LNA . We also use ^{3}H, ^{14}C and ^{36}Cl to show that artesian discharge from the underlying GAB to the LNA is locally much higher than is currently estimated from water balance models used to guide groundwater allocations in the region (Lower Namoi Groundwater 2008).

In this study we are not attempting to determine groundwater ages for all sampling locations, as it is very difficult to obtain meaningful ages for samples where significant mixing of old and recent groundwater has occurred. However, we do present "age" constraints for both modern and old end-members as a basis for delineating the relative ages of these end-members. Our results highlight the need to consider a multi-tracer geochemical approach when assessing artesian contributions to alluvial aquifers and constraining water balance models of alluvial systems globally.

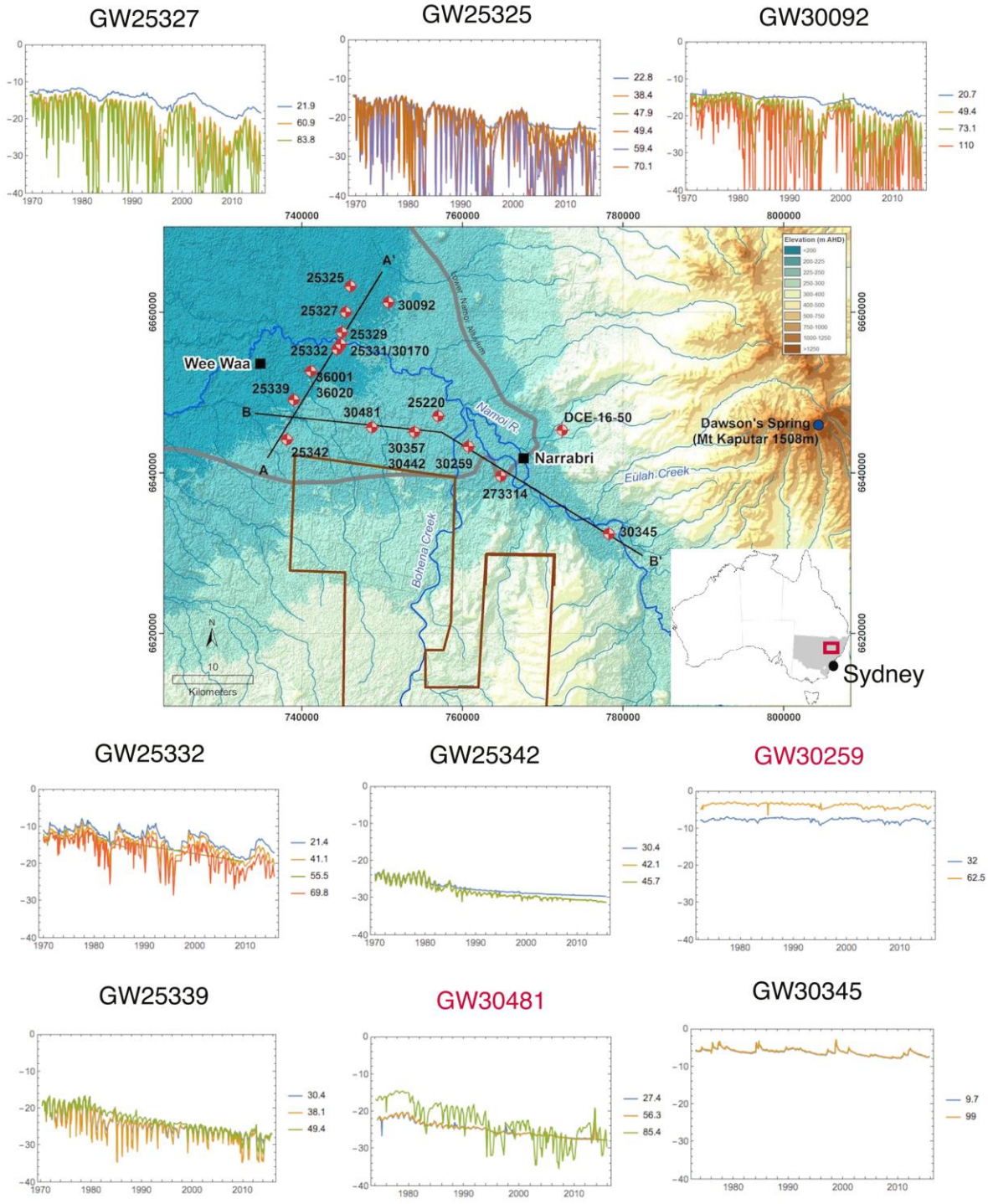

Figure 1. Map of the study area and sample locations, along with the location of the study area in Australia. Accompanying hydrographs show the groundwater level response in different piezometers throughout the study area (groundwater level data sourced from BOM 2017). The different colours in the hydrographs represent the different monitoring bores in the nested set. The bottom of the slotted

interval for each bore is shown in the key. The x-axis in each hydrograph is the year (1970-2010) and the y-axis is depth (between 0 and 40 m below ground surface (bgs)). The two locations with red text highlight areas where the hydrograph heads show clear GAB contribution, with the deeper piezometer showing a higher head than the shallow one. The remaining locations show no apparent GAB contribution to the LNA based on the hydrograph data.

2 Study Area

The lower Namoi River catchment is located in the north-west of NSW, Australia (Figure 1). Groundwater resources in the LNA are the most intensively developed in NSW (DPI Water 2017). For this reason, there is concern regarding groundwater exploitation and threat to the long-term sustainability of the system (Lower Namoi Groundwater 2008; DPI Water 2017). Groundwater abstraction from the LNA supports a multibillion-dollar agricultural sector (focused around cotton growing established in the 1960s), supplying around 50% of water for irrigation in the region (Powell et al. 2011). Peak extraction of approximately 170,000 mega litres (ML) occurred over the 1994/1995 growing season (Smithson 2009). Consistently declining groundwater levels and concern regarding the long-term sustainability of groundwater abstraction led to the implementation of a Water Sharing Plan in 2006, which systematically reduced groundwater allocations to the irrigation sector over a ten-year period. The present allocation is 86,000 ML/a (Lower Namoi Groundwater 2008).

2.1 Hydrogeological setting

The lower Namoi River catchment lies within the Murray-Darling Basin, overlying the Coonamble Embayment, which is in the south-east portion of the GAB (Radke et al. 2000). The southernmost portion of the LNA is underlain by Triassic formations, while northwest of monitoring bore 30345 the LNA is underlain by Jurassic formations (Figure 2). Within the region of study, the oldest outcropping bedrock formation is the early Triassic Digby

147 Formation (lithic and quartz conglomerates, sandstones and minor finer grained sediments)
148 (Tadros 1993). The Digby Formation outcrops in the south-east of the area and the Namoi
149 River abuts the formation just south of B' on Figure 2. The Digby Formation is overlain by
150 the Triassic Napperby Formation (thinly bedded claystone, siltstones and sandstone). This
151 formation occurs at a depth of 106 m, just below the base of monitoring bore 30345 (NSW
152 Pinneena Groundwater Database, driller logs).In outcrops to the east of the study area, the
153 Napperby Formation is overlain by the late Triassic Deriah Formation (green lithic sandstone
154 rich in volcanic fragments and mud clasts) (Tadros 1993). The boundary between the Triassic
155 and Jurassic lies west of monitoring bore 30345. The Jurassic formations important to this
156 study are the Purlawaugh Formation (carbonaceous claystone, siltstone, sandstone and
157 subordinate coal), Pilliga Sandstone (medium to coarse quartzose sandstone) and the Orallo
158 Formation (clayey to quartzose sandstone, subordinate siltstone and conglomerate) (Tadros
159 1993). The Pilliga Sandstone forms the bedrock below monitoring bores 25325 to 25342, and
160 in the Namoi region is the primary aquifer of the GAB.

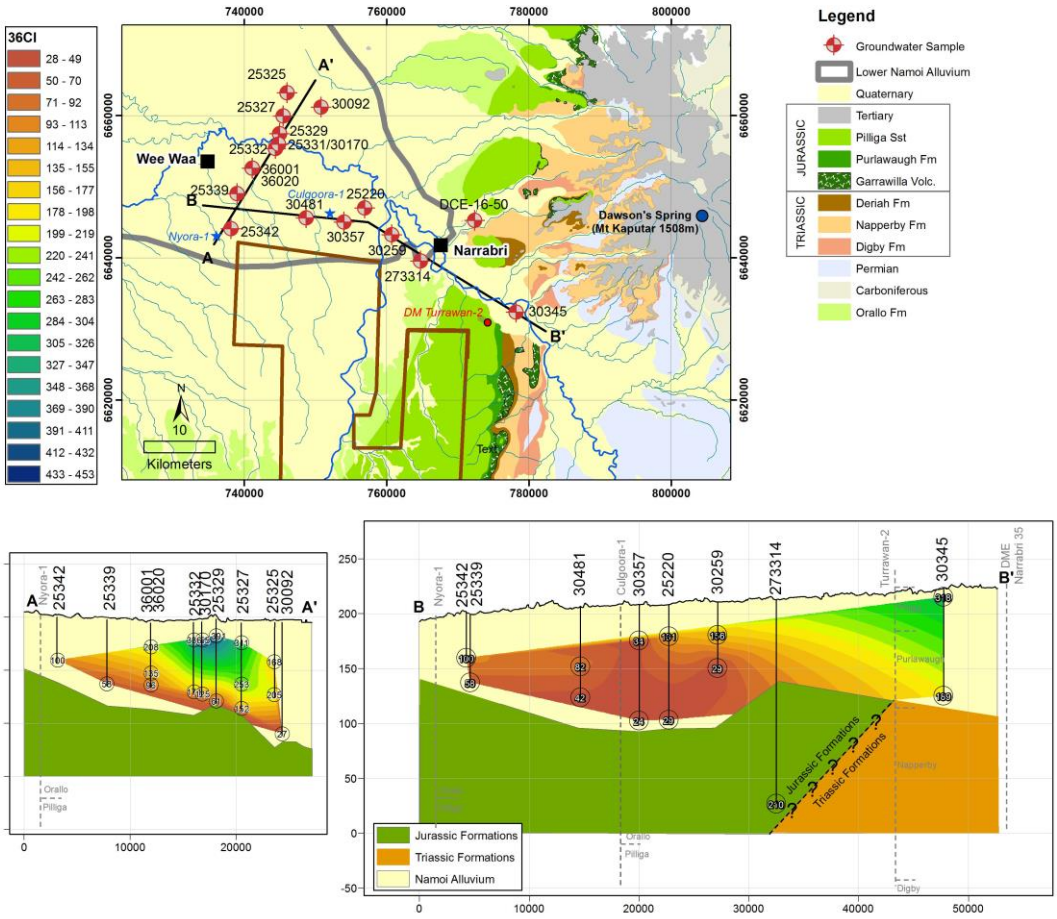

Figure 2. Two cross sections through the study area, showing the location and depth of the samples in the alluvium and their proximity to formations of the GAB. Contacts obtained from gas wells Nyora-1, Culgoora-1 and Turrawan-2, coinciding with our cross sections, are added. Their locations are displayed on the map. The chlorine-36 data interpolated using the 'natural neighbours' algorithm is shown in each cross section.

From the late Cretaceous to the mid Miocene, a palaeovalley was carved through the basement rocks (Kelly et al. 2014). Then from the mid Miocene until present, the palaeovalley was filled with reworked alluvial sediments. Groundwater abstraction in the study area is mostly from these alluvial sediments. Fluvial and aeolian interbedded clays, silts, sands and gravels form the up to ~ 140 m thick alluvial sequence of the Lower Namoi Catchment

(Williams et al. 1989). Traditionally, three main non-formally defined aquifers/formations have been used to describe the LNA. The semi-confined Cubbaroo Formation overlies the bedrock in the northern palaeochannel (which passes beneath monitoring bores 25325 and 30092). This formation is up to 60 m thick. The Cubbaroo Formation is overlain by the semi-confined Gunnedah Formation, which is up to 80 m thick, and is conformably overlain by the unconfined Narrabri Formation, which is 10 to 40 m thick (Williams et al. 1989). However, recent studies in the Namoi Catchment suggest that the rigid subdivision in to the Narrabri, Gunnedah, and Cubbaroo formations cannot easily explain the continuum in chemical evolution observed (discussed further below) and that the valley filling sequence is better characterised as a distributive fluvial system (Kelly et al. 2014, Acworth et al. 2015).

Groundwater drains from the Upper Namoi into the LNA via a bedrock constriction north of Narrabri and generally flows from east to west within the LNA (Barrett 2012). Hydraulic conductivity in the alluvial aquifer is highly variable (0.008-31 m/day) due to the presence of variable sand and clay (Golder Associates 2010). However, hydraulic conductivity generally increases with depth.

2.2 Current understanding of recharge and discharge processes in the Lower Namoi Alluvium

There have been numerous catchment water balance models and hydrochemical investigations in the study area because of the local and national economic importance of the LNA. However, the hydrochemistry of the groundwater in the region has not been used in conjunction with water balance modelling prior to this study (Merrick 2000; CSIRO 2007; Kelly et al. 2007).

2.2.1 Water balance modelling of recharge

To guide groundwater allocations from the LNA, a series of water budget models were developed using MODFLOW (Merrick 2000; summarised in Kelly et al. 2007). These models were driven by climatic, rainfall, flood and streamflow data and calibrated to groundwater head data. There are multiple plausible solutions for all water balance models and the solution presented is often constrained by several factors. These constraining factors include geological insights; the modeller's experience and biases (such as, for example, the way diffuse recharge is modelled either as a percentage of rainfall (Merrick 2000; CSIRO 2007) or as a complex evapotranspiration function (Giambastiani et al. 2012)); verification measures and pragmatic goals. One MODFLOW derived water balance model proportioned the recharge for the water budget period 1980-1994 as following: flood and diffuse rain recharge 24,100 ML/a, stream recharge 33,700 ML/a, up gradient alluvial inflow 3,060 ML/a, and artesian (GAB) recharge 9,500 ML/a. In that model, artesian recharge was inferred to occur in the eastern portion of the model (between Narrabri and Wee Waa), which overlaps with this study area (Figure 1). The zone between Narrabri and Wee Waa accounted for 42,700 ML/a of the total recharge to the LNA. Thus, according to the model, GAB discharge into the LNA in this area equated to 22%. When the LNA MODFLOW model was calibrated there was no consideration given to using hydrochemical data to constrain the calibration (Merrick 2000;CSIRO 2007; Kelly et al. 2007).

2.2.2 Hydrochemical estimates of recharge

The first isotopic investigation in the area was conducted from 1968 to 1975 and partially published by Calf (1978). The author used ^{14}C and ^{3}H to assess recharge pathways to the LNA and found evidence for river recharge in the upper aquifer, and that modern groundwater penetrated the deeper parts of the LNA. Calf (1978) also found evidence for

223 ‘leakage’ of groundwater from the GAB up into the deeper LNA, however volumetric
224 estimates were not provided.

225 McLean (2003) conducted an extensive hydrochemical and isotopic characterisation of
226 both the GAB groundwater and the alluvial groundwater in 1999-2000. This research
227 concluded that mixing of groundwater from the GAB into the lower and middle parts of the
228 LNA is an important process especially in the south of the catchment. This study also did not
229 quantify the amount of mixing occurring between the two groundwater sources.

230 The over-reliance of water balance models used to allocate groundwater resources that
231 have not been constrained by isotopic tracer residence times or hydrochemical results is a
232 common issue globally. This research highlights that hydrochemical investigations improve
233 our conceptual understanding of recharge pathways and that such investigations should be
234 applied to all important groundwater resource assessments to enable sustainable management.

235

236 **3 Materials and methods**

237 **3.1 Groundwater collection**

238 This study comprised two field campaigns, the first one from 28 January 2016 to 8 February
239 2016 (summer) when the aquifer was stressed by pumping for irrigation, and the second from
240 21 June 2016 to 30 June 2016 (winter) in the absence of abstraction for irrigation.

241 In summer, 28 groundwater samples were collected from NSW Department of Primary
242 Industries Water (DPI Water) monitoring bores and a surface water sample from the Namoi
243 River. In winter, 16 groundwater samples were collected from NSW DPI Water monitoring
244 bores and surface water samples from the Namoi River and 2 upstream tributaries (see
245 Supplementary Table 2 for locations). The bores are screened at varying intervals, intersecting
246 the shallow, middle and deep alluvium. Most bores were sampled with either a Grundfos (MP1
247 sampling pump) or Bennett compress air piston pump, with the pump placed ~ 1 m above the

248 screen when using the Grundfos pump and a drop-tube extension adjusted to place the pump
249 intake within the screen when using the Bennett pump. Some deep monitoring bores were
250 sampled with a portable bladder pump using low-flow methods (Puls & Barcelona, 1996). In
251 these bores the pump was placed approximately 10 m below standing water level, with a drop-
252 tube cut to place the pump intake within the screen. For shallower bores (less than 50 m), a 12
253 V battery operated pump was used with the pump intake placed ~1 m above the screen. For all
254 sample sites, physico-chemical parameters (pH, DO, EC) were monitored and samples
255 collected once three well volumes had been pumped and/or the physico-chemical parameters
256 stabilised. This was generally achieved within 1 to 3 hours after onset of pumping. Sample
257 collection involved an in-line, 0.45 μm, high-volume filter connected to a high density
258 polyethylene (HDPE) tube. Total alkalinity concentrations (field alkalinity) were determined in
259 the field by acid titration using a HACH digital titrator and external pH meter control. The Fe^{2+}
260 and HS^- concentrations were determined using a portable colorimeter (HACH DR/890).

261 Samples for anion and water stable isotope (δ^2H and $\delta^{18}O$) analyses were collected in 60
262 mL and 30 mL HDPE bottles, respectively, with no further treatment. Samples for cation
263 analysis were collected in 60 mL HDPE bottles and acidified with ultrapure nitric acid.
264 Samples for ^{14}C and ^{3}H were collected in 1 L narrow mouth HDPE bottles and 2 L HDPE
265 bottles respectively, and were sealed with tape to avoid potential atmospheric exchange during
266 storage. Samples for ^{36}Cl were collected in 1 L narrow mouth HDPE bottles with no further
267 treatment. Major ion and ^{14}C samples were refrigerated at 4^oC until analysed.

268 For both sampling campaigns, we aimed to collect samples representative of the river,
269 the alluvium and the GAB, however we were not able to access any previously characterised
270 GAB bores within the study area, with the only bore screened within the Pilliga Sandstone
271 (273314) (Figure 2). To better constrain GAB groundwater characteristics, we reviewed
272 regional information and used geochemical data from known GAB bores collected by Radke

et al. (2000) and McLean (2003). These data were collected to the northwest of our study area and are used as a range (depending on availability of the original reported data) for the GAB end-member in all future plots and discussions (Supplementary Table 1).

To help in the description of results, we use shallow (< 30 m), intermediate (30 – 80 m) and deep (> 80 m) as a rough guide to the origin of the groundwater sample. The chosen depth categories are based on clusters and trends in the ^{14}C analyses. Groundwater samples from similar contemporaneous alluvial-filled valleys in other eastern Australian river valleys show a continuum of geochemical evolution that cannot be explained by separating samples into arbitrary aquifers (such as the aforementioned Narrabri, Gunnedah and Cubbaroo Formations). In such settings, proximity to modern channels and depth are the primary controls on residence time (Cendón et al. 2010; Iverach et al. 2015).

3.2 Geochemical analyses

Groundwater samples from both campaigns were analysed at ANSTO by inductively coupled plasma atomic emission spectroscopy (ICP-AES) for cations and ion chromatography (IC) for anions. Samples for δ^2H and $\delta^{18}O$ were analysed using Cavity Ring-Down Spectroscopy (CRDS) on a Picarro L2130-*i* analyser. These values are reported as ‰ deviations from the international standard V-SMOW (Vienna Standard Mean Ocean Water) and results are accurate to ± 1‰ for δ^2H and ± 0.15‰ for $\delta^{18}O$.

The ^{14}C samples were processed and analysed at ANSTO using methods described in Cendón et al. (2014). The ^{14}C activities were measured by accelerator mass spectrometry (AMS) using the ANSTO 2MV tandetron accelerator, STAR (Fink et al. 2004). The ^{14}C results were reported as percent modern carbon (pmc) following groundwater ^{14}C reporting criteria (Mook & van der Plicht 1999; Plummer & Glynn 2013) with an average 1σ error of 0.21 pmc.

297 The ^{3}H samples were analysed at ANSTO. Water samples were distilled and
298 electrolytically enriched prior to analysis by liquid scintillation. The ^{3}H concentrations were
299 expressed in tritium units (TU) with a combined standard uncertainty of ± 0.03 TU and
300 quantification limit of 0.04 TU. Tritium was measured by counting beta decay in a liquid
301 scintillation counter (LSC). A 10 mL sample aliquot was mixed with the scintillation cocktail
302 that releases a photon when struck by a beta particle. Photomultiplier tubes in the counter
303 convert the photons to electrical pulses that are counted over 51 cycles for 20 minutes.
304 The $^{36}Cl/Cl$ and $^{36}Cl/^{37}Cl$ ratios were measured by AMS using the ANSTO 6MV SIRIUS
305 Tandem Accelerator (Wilcken et al. 2017). Samples were processed in batches of 10, with
306 each batch containing 1 chemistry blank. The amount of sample used was selected to yield ~
307 5 mg of Cl for analysis without carrier addition. Chloride was recovered from the sample
308 solutions by precipitation of AgCl from hot solution (Stone et al. 1996). This AgCl was re-
309 dissolved in aqueous NH_3 (20-22 wt %, IQ grade, Seastar) to remove sulfur compounds of Ag.
310 Owing to isobaric interference of ^{36}S with ^{36}Cl in the AMS measurements, a saturated
311 $Ba(NO_3)_2$ solution (99.999% trace metal basis) was used to precipitate sulfur as $BaSO_4$. At
312 least 72 h were allowed for $BaSO_4$ to settle from a cold solution (4℃) in the dark before
313 removal of the supernatant by pipetting and filtration (0.22 Millex GS). Pure AgCl was re-
314 precipitated by acidifying the $Ag(NH_3)_2$-Cl solution with 5M nitric acid (IQ Seastar, sub-
315 boiled). Finally, AgCl was recovered, washed twice and dried. It was then pressed into high-
316 purity AgBr (99% trace metal basis, Aldrich) in 6 mm diameter Cu-target holders. AgBr has a
317 much lower sulfur content than Cu. The stable Cl isotopes ^{35}Cl and ^{37}Cl were measured with
318 Faraday cups and ^{36}Cl events were counted with a multi-anode gas ionisation chamber. Gas
319 (Ar) stripping (for good brightness/low ion straggling) the ions to 5+ charge state in the
320 accelerator terminal suffices for effective ^{36}S interference separation in the ionisation chamber
321 combined with sample-efficient and rapid analysis. Purdue PRIMELab Z93-0005 (nominally

322 $1.20x10^{-12}$ $^{36}Cl/Cl$) was used for normalisation with a secondary standard (nominally $5.0x10^{-13}$
323 $^{36}Cl/Cl$ (Sharma et al. 1990)) used for monitoring. Background subtraction was done with a
324 linear dependence between ^{36}Cl-rate and interfering ^{36}S-rate. This dependency is established by
325 combining all the blank and test sample measurements and applied to the unknown samples
326 during offline data analysis. This correction factor was typically less than analytical uncertainty
327 of 3-4% bar one sample that had a correction factor of 12% with an analytical uncertainty of
328 6%.
329
330 **3.3 Geochemical calculations**
331 Calculations necessary to assess electrical neutrality, dissolved element speciation and
332 saturation indices for common mineral phases were undertaken using the PHREEQC
333 Interactive program (3.3.8) (Parkhurst & Appelo 1999) and the incorporated WATEQ4F
334 thermodynamic database (Ball & Nordstrom 1991). The cation and anion analyses were
335 assessed for accuracy by evaluating the charge balance error percentage (CBE%). All samples
336 fell within the acceptable ± 5% range, except for samples 25327-1 and 36001-1, which both
337 contained high NH_4^+ concentration that was not part of the initial ion analyses. This elevated
338 NH_4^+ concentration skewed the CBE% so that they were initially outside the acceptable ± 5%
339 range. The inverse geochemical modelling code NEPATH XL (Plummer et al. 1994; Parkhurst
340 & Charlton 2008) has been used to calculate the mixing ratio between two end-members, using
341 their Cl concentrations. The choice of end-members will influence calculated proportions.
342 However, end-members were selected to provide conservative approximations. In general, Cl
343 concentrations in surface water and shallow groundwater in the study area are low (< 30 mg/L),
344 while samples recovered from the Pilliga Sandstone (GAB) have higher concentrations (~ 60
345 mg/L). We mix a representative shallow, modern groundwater (30170-1) with an average GAB
346 composition obtained from regional groundwater samples (McLean 2003). These two initial

end-members are mixed in different proportions so that Cl concentrations in a selected final bore can be explained via inverse modelling calculations.

^{36}Cl residence times were calculated from the equations of Bentley et al. (1986), assuming no other sources or sinks besides recharge and natural decay (eqn. 1):

$$t = \frac{-1}{\lambda_{36}} \ln \frac{R - R_{se}}{R_0 - R_{se}} \quad (1)$$

where R = ^{36}Cl/Cl ratio measured in the sample, R_0 = the initial ^{36}Cl/Cl ratio (meteoric water), R_{se} = the ^{36}Cl/Cl ratio under secular equilibrium (in this case the ^{36}Cl/Cl ratio from the Pilliga Sandstone), and λ_{36} is the decay constant (2.303 x 10^{-6}). We used a R_0 value of 160 (x10^{-15}), which was an average of 10 samples compiled from studies in the Coonamble Embayment and reported in Radke et al. (2000). For R_{se} a value of 5.7 (x10^{-15}) was used, which is appropriate for aquifers dominated by sandstone (this secular equilibrium value can vary according to the dominant lithology). This R_{se} value has been applied to ^{36}Cl/Cl calculations elsewhere in the GAB (Moya et al. 2016).

4 Results

4.1 Major ion chemistry

The groundwater of the alluvial aquifer is predominantly Na-HCO_3-type water, with concentrations ranging from 0.12 mmol/L to 54.6 mmol/L (average: 6.85 mmol/L) for Na^+ and 0.29 mmol/L to 24.0 mmol/L (average: 6.43 mmol/L) for HCO_3^- (Supplementary Table 2). Generally, the highest concentrations of Na^+ and HCO_3^- occur in the deeper groundwater and decrease up the vertical groundwater profile (Figure 3a). The concentration of these two ions in the groundwater of the LNA is higher than expected from local rainfall sources and other shallow groundwater alluvial systems in eastern Australia (Martinez et al. 2017). In GAB groundwater, the Na-HCO_3 molar ratio is generally 1:1 and the two ions are generally

present in higher concentrations than in our alluvial samples (Radke et al. 2000; McLean 2003), which is evident in the position of the regional GAB samples in Figure 3a.

Additional ions used in this study are F^-, Cl^- and the Cl/Br ratio. The concentration of F^- in the groundwater ranges from 0.002 mmol/L to 0.215 mmol/L (average: 0.028 mmol/L). Fluoride concentrations generally increase with depth and accumulate in solution as all groundwater samples are below saturation with respect to fluorite (Figure 3b). Concentrations of Cl^- in the alluvial groundwater range from 0.063 mmol/L to 26.73 mmol/L (average: 1.67 mmol/L). Unlike the other major ions, Cl^- concentrations through the vertical groundwater profile are relatively stable (Figure 3c). The relationship between Cl^- and the Cl/Br ratio shows that groundwater composition clusters from values below the seawater ratio to values close to seawater. The Cl/Br ratios are similar to ranges found in other alluvial groundwater systems but slightly lower than ratios observed in other GAB samples for Australian locations (Herczeg et al., 1991; Cendón et al., 2010; Cartwright et al., 2010). Additionally, the Cl/Br ratios in shallow samples connected to the river are consistent with expected ratios in rainfall (Short et al. 2017). The regional GAB samples (Radke et al. 2000) show a Cl/Br ratio more similar to seawater, with our samples from the LNA lying on a mixing trend between the two end-members (Figure 3c).

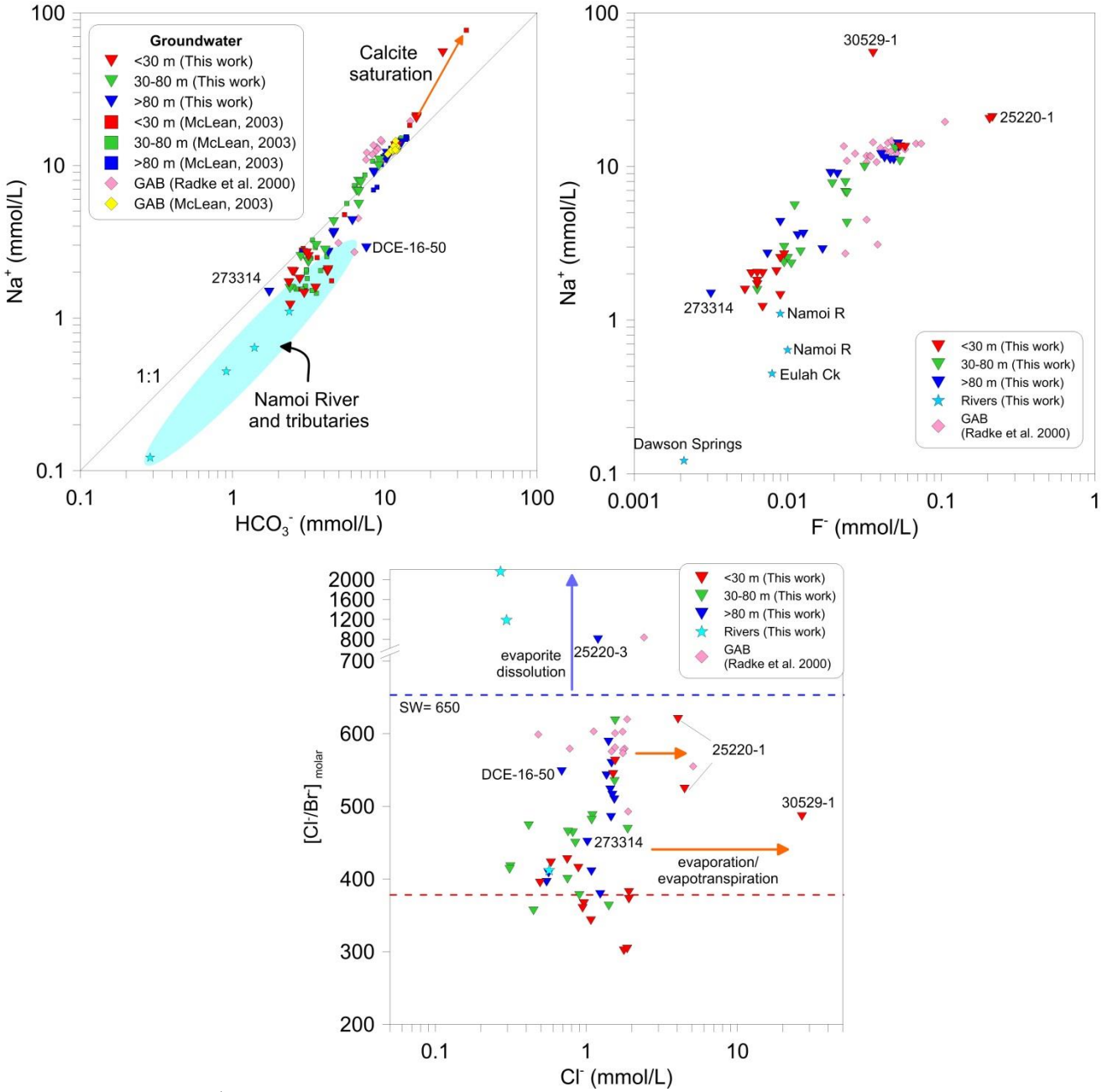

389 **Figure 3.** a) Na^+ vs HCO_3^- showing the mixing trend that the alluvial samples form between the
390 Namoi River and samples from the GAB (Radke et al. 2000; McLean 2003). The shaded blue ellipse
391 represents all river chemistry data available for the Namoi River and tributaries (this work (n=4),
392 McLean 2003 (n=4), Mawhinney 2011 (n=79)); b) Na^+ vs F^- and c) Cl^-/Br^- vs Cl^-, highlighting the
393 mixing trend between the surface recharge and the GAB that we observe in other geochemical
394 indicators. The red dotted line represents the Cl^-/Br^- ratio for rainfall and the blue dotted line is the
395 seawater ratio.
396

We identified one major outlier in the hydrochemical results, which was sample 273314. This sample is from 207 m bgs and the bore screen is classified as being in the GAB. However, the geochemical parameters for this deep GAB sample have a signature more similar to river water than what would be expected in the GAB 207 m bgs. The concentration of Na^+, HCO_3^-, Cl^-, F^- and the Cl/Br ratio in this sample plot closer to the river and shallow groundwater than the deeper groundwater system (Figure 3). Potential reasons for this are explored in detail below.

4.2 Water stable isotopes (δ^2H and $\delta^{18}O$)

The stable water isotopic values for this study range from -0.76‰ to 8.4‰ for $\delta^{18}O$ and -7.5‰ to -54.9‰ for δ^2H. Most groundwater samples cluster together at around -6‰ and -40‰ ($\delta^{18}O$ and δ^2H) and lie on the global meteoric water line (GMWL), to the right of the nearest available local meteoric water lines (LMWL) (Macquarie Marshes and Gunnedah) (Figure 4; Supplementary Table 3). A group of mostly shallow samples collected from piezometers close to river channels follow an evaporation line. Our results are similar, including the shallow groundwater evaporative trend, to those recorded by McLean (2003). Water stable isotopic compositions for regional GAB samples range from -6.58‰ to -6.24‰ for $\delta^{18}O$ and -43.1‰ to -38.8‰ for δ^2H (McLean 2003) (Figure 4).

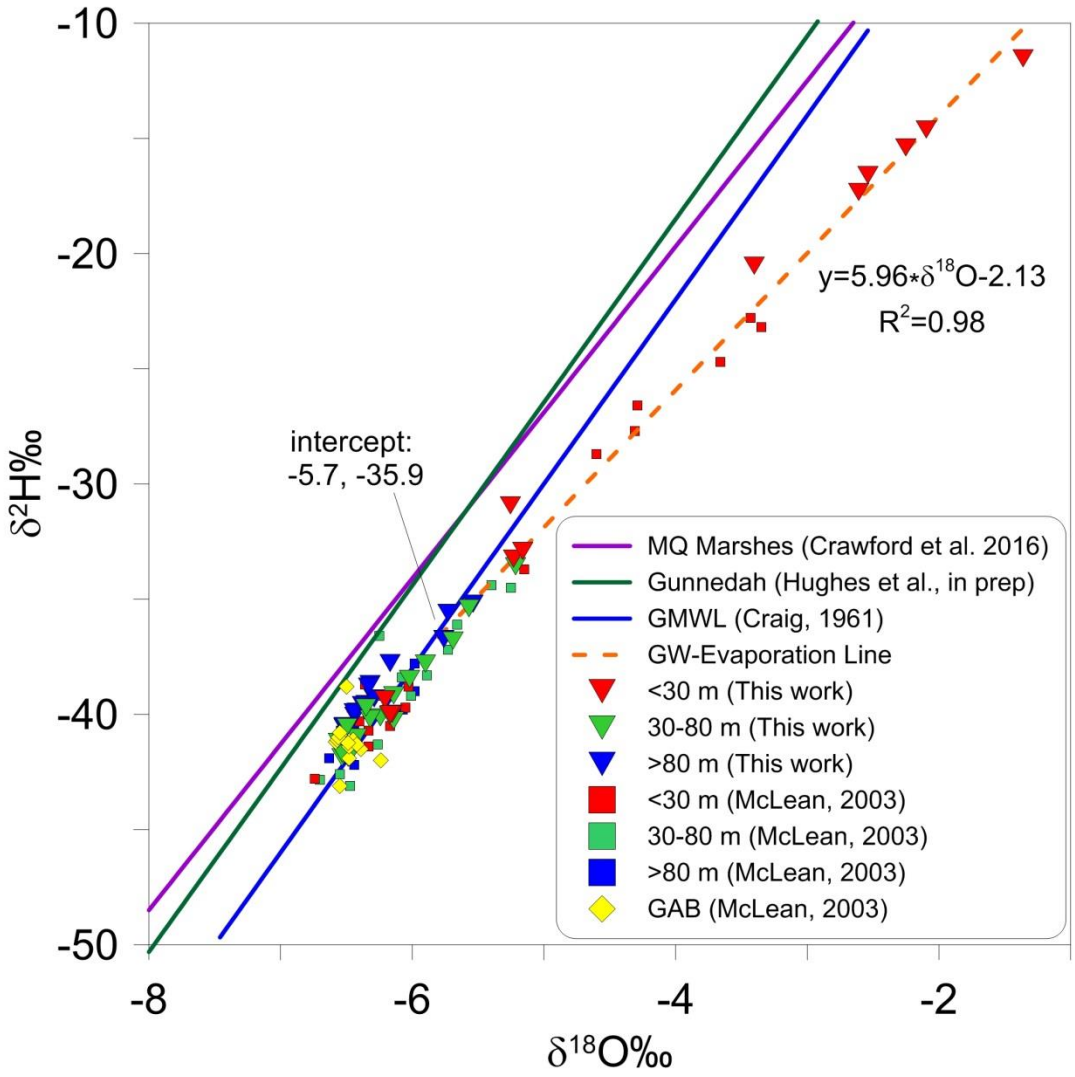

Figure 4. Water stable isotopes in the LNA, showing the two separate mechanisms of recharge; surface water recharge plotting along an evaporation trend line and potential inflow from the GAB clustered with regional samples from the GAB (McLean 2003).

4.3 Isotopic tracers (^{3}H, ^{14}C and ^{36}Cl)

Tritium activities vary throughout the study area, ranging from 0.01 TU to 2.36 TU (average: 0.42 TU). Tritium activities generally decrease with depth and distance from the river channel (Figure 5) (all data in Supplementary Table 3), with modern recharge evident in the high ^{3}H activities near the main river channels. However, ^{3}H above the detection limit (0.04

TU) was measured at depth (down to 207 m bgs). The ^{3}H activities we measured at depth are significant for Australian groundwater, as the peak of the bomb pulse in Australia was around 60 TU and ^{3}H in Australian rainfall as been at natural background concentrations for some time.

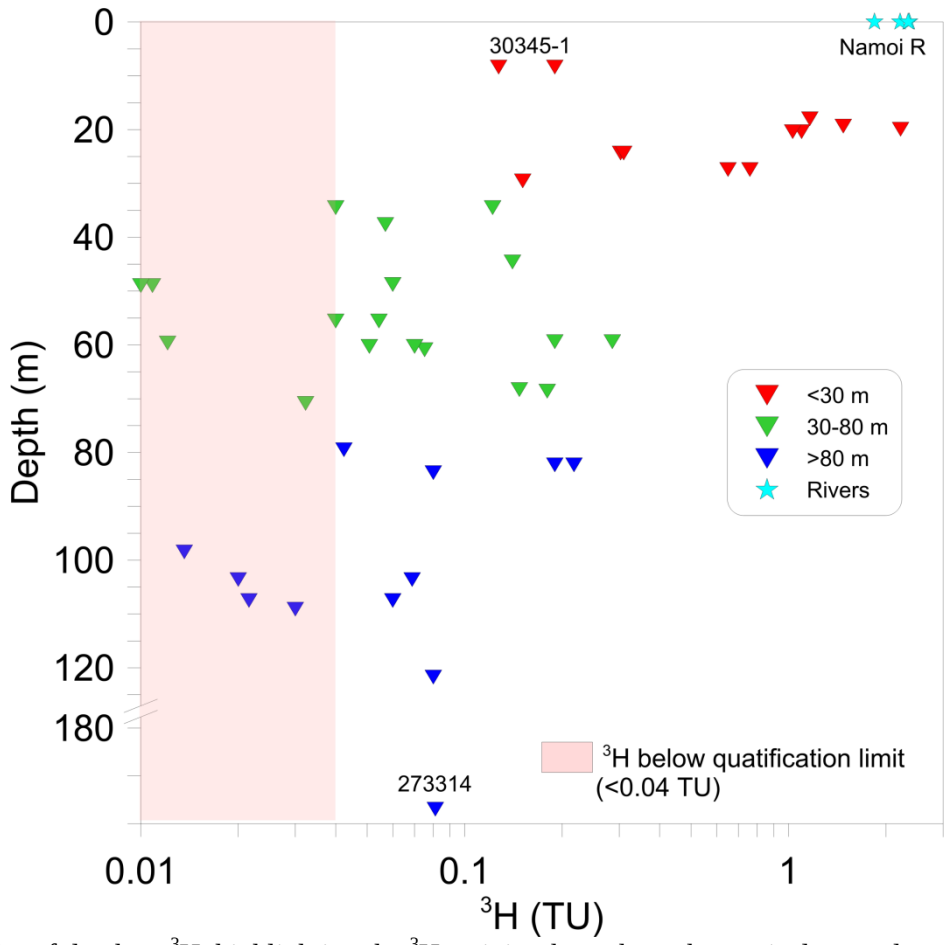

Figure 5. Plot of depth vs ^{3}H, highlighting the ^{3}H activity throughout the vertical groundwater profile.

The ^{14}C content in the groundwater ranged from 0.2 pmc to 107.6 pmc (average: 54.0 pmc). Generally, groundwater samples shallower than 30 m had a high ^{14}C content (> 90 pmc), which decreased with depth. There were 9 samples with a ^{14}C content below 1 pmc, indicating very old groundwater (> 30 ka), with total depths ranging from 35 m bgs to 207 m bgs.

Our ^{36}Cl results for the alluvial groundwater ranged from 24.06 ($x10^{-15}$) to 455.35 ($x10^{-15}$) (average: 169.4 ($x10^{-15}$) (shown in the interpolation in Figure 2). It has been found that groundwater in the GAB recharge zone closest to the study area has a $^{36}Cl/Cl$ ratio up to ~ 200 ($x10^{-15}$) (Radke et al. 2000) with recharge values applied in calculations elsewhere in the GAB of 110 ($x10^{-15}$) (Moya et al. 2016). Water from the Namoi River has a $^{36}Cl/Cl$ ratio of ~ 420 ($x10^{-15}$), possibly affected by thermonuclear ^{36}Cl input from atmospheric bomb testing in the 1950s (Supplementary Table 4).

5 Discussion

5.1 Identification of recharge and mixing between the GAB and the LNA

The $\delta^{18}O$ and $\delta^{2}H$ isotopic compositions suggest two mechanisms of recharge to the alluvium: artesian discharge and surface water infiltration. The regional GAB samples plot within the alluvial groundwater sample range, suggesting a GAB component in the alluvium. The evaporation line in Figure 4 indicates recharge to the alluvium via surface water infiltration. It also shows a good connection between surface water that has undergone evaporation and shallow groundwater.

Additional evidence for these two mechanisms of recharge is the composition of Na^+ and HCO_3^- in the LNA. Figure 3a shows a mixing line that the alluvial samples follow, plotting between the end-members of the GAB and the Namoi River, suggesting an increasing GAB contribution to the alluvial groundwater with depth. This also implies that a continuum of mixing exists between the shallow and deep groundwater within the LNA. The shallow samples (25220-1 and 30259-1) that are more Na^+ enriched compared to samples from the GAB have undergone separate evapotranspiration processes and hence have a concurrent increase in Cl^-. Assuming that Cl^- is behaving conservatively (Appelo & Postma

2005) we surmise that increases in dissolved major ion concentrations concomitant with increases in Cl^- in the shallow groundwater are likely to be a result of evaporation.

Further hydrochemical evidence for these recharge mechanisms is the covariation of Na^+ and F^-, both interpreted as primarily derived from groundwater interaction with silicate minerals in this region (Airey et al. 1978; Herczeg et al. 1991; McLean 2003) (Figure 3b). Our alluvial samples fall on the mixing line between samples from the river and nearby tributaries and regional samples from the GAB (Radke et al. 2000), in a similar way to the Na-HCO_3 trend that we observe in Figure 3a. The Cl/Br ratios in the groundwater also support the mixing interpretation provided by the Na^+ and HCO_3^- concentrations, contrary to the possibility of water rock interactions along the alluvium flowpath (Figure 3c). Furthermore, the relationship between ^{36}Cl and Na^+ provides additional evidence of mixing in the groundwater (Supplementary Figure 1).

Figure 3 also highlights the aforementioned deep outlying sample (273314), which was 207 m bgs in total depth, yet plots with the shallow alluvial and river samples. Figure 2 shows that this sample is situated just above the Napperby Formation. We hypothesise that this sample originated from surface recharge from the Namoi River (which is in contact with the underlying Digby Formation to the south of the study area), with negligible input from the more Na-HCO_3-rich groundwater in the Pilliga Sandstone, where the sample is from. Sample 30345-2 (Supplementary Tables 2 and 3), which is situated in the lower part of the LNA in proximity to the alluvial contact with the Napperby Formation (Figure 2) has a similar geochemistry. These results suggest the connection between deeper Triassic formations beneath the GAB and the Namoi River, which must be an important consideration in future water balance models of the catchment.

5.1.1 Mixing between groundwaters of varying residence times

Major ion and water stable isotope data suggest two primary mechanisms of recharge to the LNA and show that mixing is occurring within the alluvium. ^{3}H activity and ^{14}C content in the alluvial groundwater to quantify the potential residence times of the groundwater sources that are mixing within the alluvium. Tritium activities above the detection limit at depth (down to 207 m bgs) indicates the extent of recharge from episodic flooding. Measuring ^{3}H above the detection limit at these depths also shows that surface recharge reaches the deeper LNA relatively quickly (< 70 years). Past ^{3}H data from the region (Calf 1978) suggest that ^{3}H was already present in the deeper parts of the alluvial aquifer (> 70 m bgs) prior to a major flood in 1971, with activities ranging from 7.9 TU to 11.2 TU. This indicates good connectivity to the surface. Additionally, measurements of ^{3}H post-flooding (16.6 to 20.7 TU) indicate that substantial recharge took place during this flood, highlighting the importance of surface water recharge to the LNA. The activities of ^{3}H above the detection limit throughout the vertical profile of the LNA (Figure 5) are inconsistent with the low ^{14}C contents in the groundwater. The presence of measurable ^{3}H but negligible ^{14}C (close to 0 pmc) suggests that mixing is occurring between groundwater that is associated with modern recharge processes in the alluvium and groundwater that, as indicated by the ^{14}C content, is presumably much older. This older groundwater may be derived from artesian inflow. Figure 6 shows ^{3}H activities above the detection limit in samples with ^{14}C content of almost 0 pmc, suggesting that groundwater with a very low ^{14}C content is mixing with groundwater with a high ^{3}H activity. Even though there is evidence of ^{14}C dilution in localised areas, we also observe mixing between groundwaters of widely different ^{14}C and ^{3}H values in the gradient of the samples in Figure 6 (emphasised with a dotted blue line). This gradient would be steeper if there were mixing between groundwaters closer in residence times (Cartwright et al. 2013).

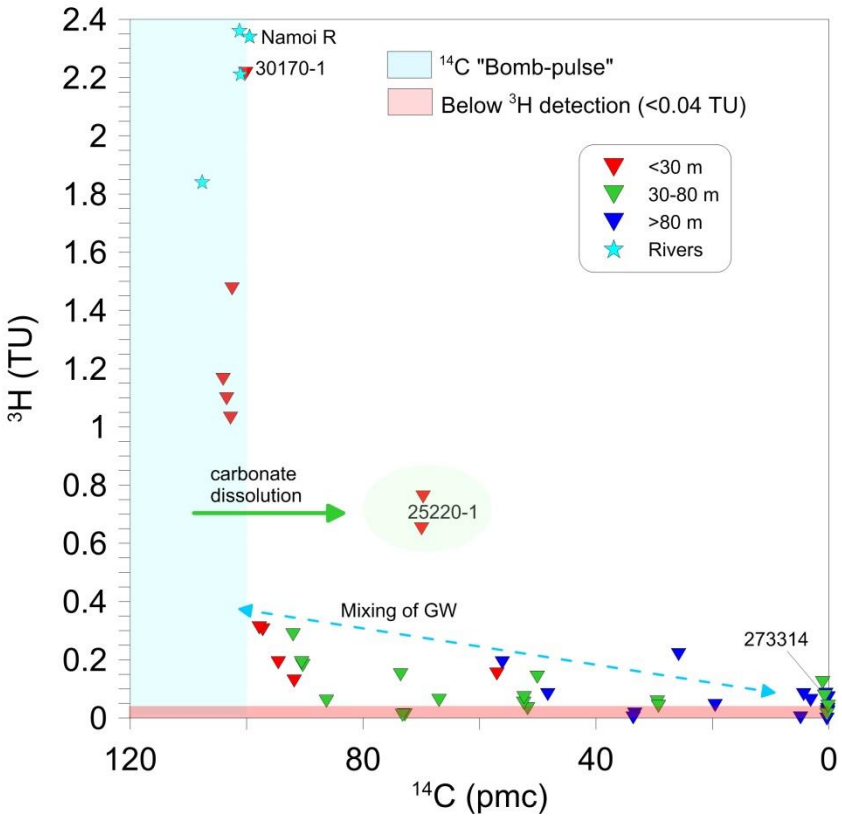

Figure 6. ^{3}H (TU) vs ^{14}C (pmc). This shows the mixing between groundwater with detectable ^{3}H activity (as indicated by the red band) and groundwater with very low ^{14}C content (as indicated by the dotted blue line).

5.2 Extent of interaction between the GAB and the LNA

The ^{3}H and ^{14}C values show that there is mixing between groundwater of varying residence times, however they provide little constraint on the groundwaters with a ^{14}C content of close to 0 pmc (ie > 30 ka). This is where chlorine-36 dating can be a useful tracer because it can be used to identify the presence of groundwaters that are much older than the range provided by ^{14}C.

A plot of $^{36}Cl/Cl$ vs ^{14}C (pmc) (Figure 7) shows a distinct mixing trend between groundwater with high and very low ^{14}C content. The 2 deep outlying samples (30345-2 and

273314; shaded yellow ellipse in Figure 7) display different geochemical characteristics from the other samples, possibly because of their aforementioned proximity to the Napperby Formation (Figure 2). Figure 7 shows the $^{36}Cl/Cl$ value range of GAB recharge, highlighting the alluvial samples with values lower than this GAB recharge value. This suggests that these alluvial groundwaters are influenced by artesian inflow of very old groundwater. This is evident in the natural neighbour interpolation in Figure 2.

The longest residence time calculated from eqn. 1 for our study area is between 700 ka and ~900 ka. Using the two extremes of the $^{36}Cl/Cl$ range for GAB recharge (100 ($x10^{15}$) and 200 ($x10^{15}$)) this calculated residence time would be slightly shorter or slightly longer, respectively.

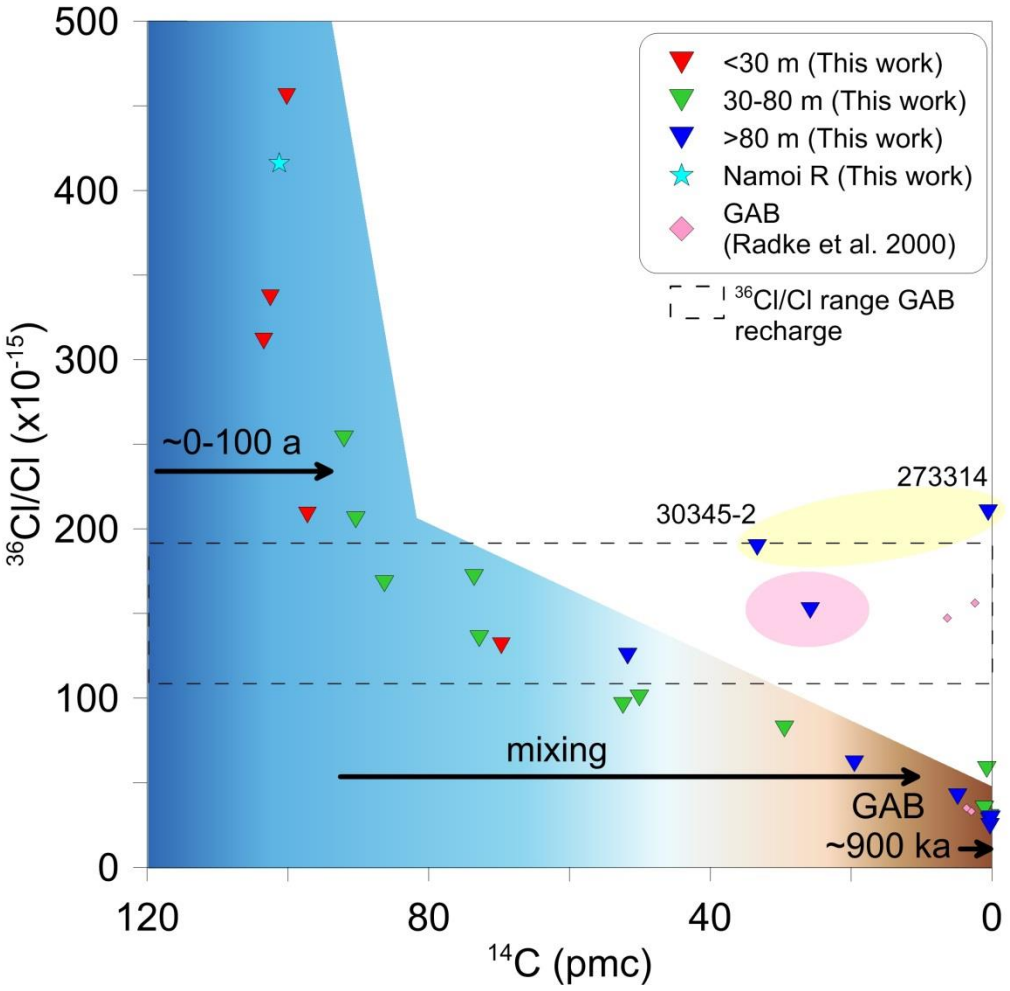

Figure 7. $^{36}Cl/Cl$ ($x10^{-15}$) vs ^{14}C (pmc). The colour gradient represents the mixing between the two major sources: surface water recharge (blue = modern) and the GAB (brown = old). The shaded

yellow ellipse encompasses the two outliers where the geochemistry is being influenced by proximity to the Napperby Formation. The shaded pink ellipse is sample 25327-3 located in the irrigation area.

The apparent degree of ^{36}Cl decay observed in the alluvial groundwater samples is too large to be explained simply by radioactive decay as indicated by the measurable ^{14}C content in the same samples (Phillips 2000). This means that the time needed for the ^{36}Cl to decay as much as observed would be well outside the range of ^{14}C dating (> 30 ka) and therefore all groundwater samples would be expected to have a ^{14}C content of 0 pmc, which is not observed. Furthermore, the decrease in ^{36}Cl is unlikely to result from dilution by ^{36}Cl-depleted sources such as evaporites, as the Cl^- concentrations are similar in most samples (Figure 8a and b). Therefore, mixing between groundwaters of different residence times is the most likely explanation for the observed ^{36}Cl signatures.

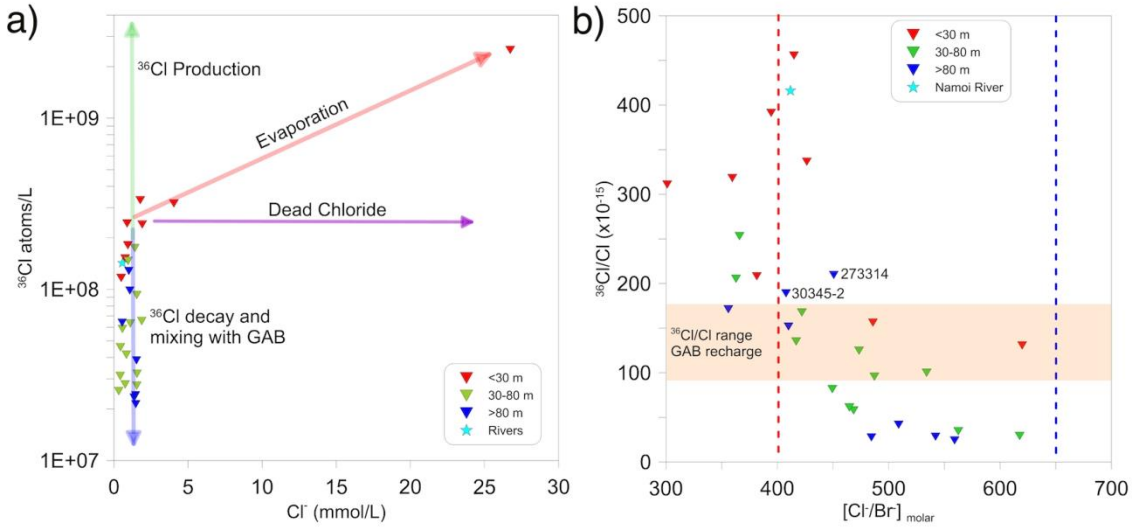

Figure 8. a) ^{36}Cl vs Cl^- concentration. The ^{36}Cl production arrow represents in situ ^{36}Cl production as a result of high U and Th in host rocks; b) $^{36}Cl/Cl$ ratio ($x10^{-15}$) vs Cl^-/Br^-. The dotted blue line represents the Cl^-/Br^- ratio in seawater and the dotted red line represents the expected Cl^-/Br^- ratio for rainfall at Narrabri based on distance from the coast (Short et al. 2017).

Our groundwater samples from the deep alluvium display lower $^{36}Cl/Cl$ ratios (down to 24 ($x10^{-15}$)) than those measured in the GAB recharge zone. This indicates that there is very old groundwater in the deeper LNA (up to 900 ka), and that the mixing observed in our geochemical data could be taking place between groundwater with a residence time of less than 70 a (assumed using ^{3}H) and groundwater with a residence time of ~ 900 ka (calculated using ^{36}Cl; an approximation based on eqn. 1). In the study area, the only source of groundwater with a residence time of ~ 900 ka is the GAB.

To quantify the extent of interaction between the two groundwater sources, we use the concentration of the conservative chloride ion to determine an approximate percentage of GAB to alluvial groundwater at each sample location. To estimate the local surface infiltration end-member, a shallow groundwater sample with a high ^{3}H activity (sample 30170-1; 2.21 TU) was used. The average of all available GAB data was used for GAB inputs. These end-members are mixed in varying proportions to obtain the Cl^- concentration that we observe in all our groundwater samples. If the Cl^- concentration in the sample was lower than that in the representative local surface infiltration sample, a 100% LNA contribution is assumed. The representative sample used as the local surface infiltration end-member has been subject to some evaporation and therefore does not have the lowest Cl^- concentration in the alluvium. If the sample with the lowest Cl^- concentration was used as the surface water end-member, we would require a higher percentage of GAB contribution across the study area. Thus, the use of the evaporated sample as our end-member represents a conservative approach when considering the mixing components from both the LNA and the GAB.

The Cl mixing results provide an approximate mixing threshold with shallower samples generally containing a higher proportion of alluvial groundwater, which diminishes with depth. These mixing proportions show that some deeper samples in the LNA contain up to

70% GAB groundwater. Figure 9 presents approximate contours for artesian discharge proportions into the LNA based on the Cl mixing approach. The dotted lines indicate areas where there is just one sample to inform the interpretation, whereas the solid lines connect multiple samples that all displayed similar contributions from the GAB.

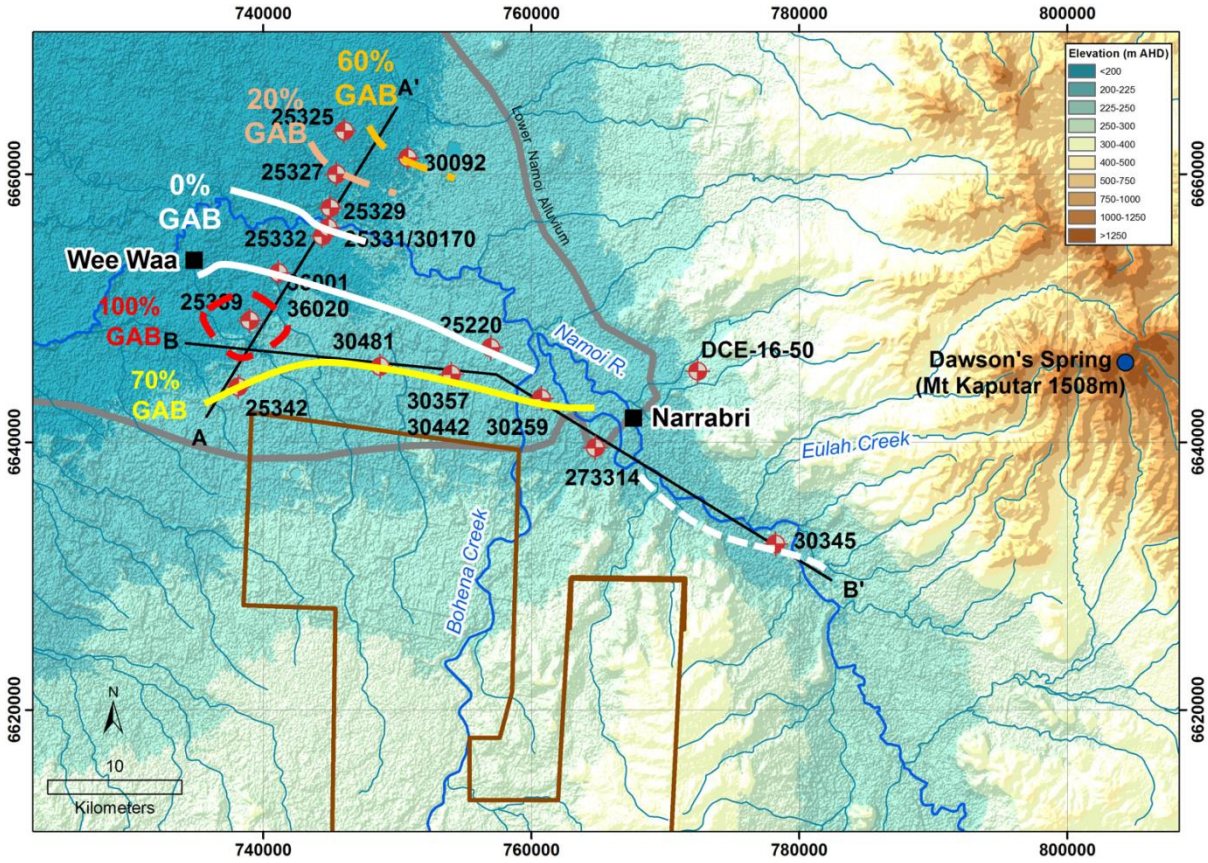

Figure 9. Approximate percentages of GAB contribution to the LNA, calculated from multiple geochemical tracers and major ion data.

Artesian input can be inferred from nested piezometers at locations 30481 and 30259 (Figure 1). At these locations, the monitoring bore slotted in the lower portion of the LNA has a head higher than the monitoring bore slotted in the shallow portion of the LNA, indicative of upward flow. At all other locations artesian contributions cannot be discerned from head data. Comparing Figure 9 to Figure 1 we show that groundwater geochemistry can provide a more accurate evaluation of GAB contribution to the LNA. Multiple geochemical

595 tracers reveal that boreholes in the north and west of the study area may be experiencing
596 much more GAB inflow than has been inferred in catchment water balance models (Merrick
597 2000; Kelly et al. 2007; CSIRO 2007). This is most evident at sample 25342. It is not
598 immediately apparent from the vertical heads in the hydrograph set at sample 25342 that
599 there is any GAB inflow, yet based on the geochemical tracers this location is 100 % GAB
600 groundwater. The water balance model described in Merrick (2000) has GAB groundwater
601 contributing 22% of all inflow into the LNA between Narrabri and Wee Waa (Figure 1).
602 From the geochemistry alone it is not possible to make an estimate that can be directly
603 compared to that artesian discharge estimate. However, it is apparent from the mixing results
604 shown in Figure 9 that a large portion of the study area has an artesian input to the LNA that
605 is likely to be greater than 22%. The above observations highlight why geochemical insights
606 should ideally be used as one of the constraining data sets when doing water balance models
607 in regions where there is both artesian discharge and surface water recharge to the alluvial
608 aquifer.
609
610 **5.3 Temporal changes in the interaction between the LNA and the GAB**
611 The multiple geochemical tracers we have used show substantial artesian discharge to the
612 LNA, which is larger than that currently considered in groundwater models of the region
613 (Merrick 2000; Kelly et al. 2007; CSIRO 2007). Time series sampling can constrain how this
614 GAB discharge changes over time and is important for understanding future artesian
615 contributions to the LNA. We use ^{14}C (pmc) data collected in 1978 (Calf), 2003 (McLean),
616 2010 (ANSTO data) and 2016 (this study) to observe how the ^{14}C content in the groundwater
617 changes over that period. Even though dissolved inorganic carbon content and isotopic
618 signature can be affected by processes involving both organic and inorganic carbon sources
619 along its flow path, (which can alter the ^{14}C content) the application of ^{14}C data can still be

620 useful as a tracer when investigating mixing and recharge processes (Meredith et al. 2016).
621 This is especially the case if it is assumed that the processes that can potentially alter the ^{14}C
622 signature do not change substantially over the period where different historical ^{14}C data are
623 compared. Therefore, the historical ^{14}C data, coupled with data from this study could be used
624 to estimate the changes in relative contributions of high ^{14}C contents from recent surface
625 recharge (~ 100 pmc) versus low ^{14}C contents of the GAB discharge to the LNA. The dataset
626 contains 14 bores from 5 nested sites and is the most comprehensive long-term time-series
627 database for the study area, if not Australia, despite not being complete for all years.

628 Most of the samples displayed relatively consistent ^{14}C values across the years where
629 data were available. However, we observed large changes in ^{14}C content in 5 monitoring
630 bores; 4 showed an increase and 1 showed a decrease (bold text in Table 1). The borehole
631 that displayed a decrease in ^{14}C (30092-2) between 2003 and 2016 suggests that there is an
632 increasing GAB contribution over the time period at this site. Using the Cl^- concentration,
633 this sample displayed 60% GAB contribution (Figure 9), despite the vertical head gradients
634 in the hydrograph showing no evidence of this (Figure 1). The remaining 4 monitoring bores,
635 primarily located deeper in the LNA, have an increase in ^{14}C, suggesting a larger alluvial
636 contribution at these locations over time. At monitoring bore 25332-4, ^{14}C increased between
637 1978 and 2010, then decreased between 2010 and 2016. These locations were in the northern
638 part of the study area where there is extensive pumping for irrigation, suggesting that these
639 changes in the ^{14}C contents are reflecting the extent of pumping occurring and associated
640 surface water recharge with modern carbon versus artesian discharge. Therefore, measuring
641 the ^{14}C in the groundwater at any future time and assessing how this has changed using past
642 data is useful as a preliminary indicator for the current state of the system.
643

Table 1. Changes in ^{14}C content (pmc) in select boreholes in the study area between 1978-2016 (see Figures 1 and 8 for the locations of the bores). The 5 bores in bold text highlight where we observe changes in the ^{14}C content from 1978 to this study. Where available, the time of sampling is included. ND = no data.

Bore	Depth interval (m bgs)	Calf (1978)	McLean (2003)	ANSTO data (summer 2010)	This study (summer 2016)	This study (winter 2016)
25220/1	**24.4-30.5**	**28.15**	**ND**	**ND**	**69.66**	**69.94**
25220/3	97.5-109.7	0.99	ND	0.13	0.17	0.22
25325/2	36.9-38.4	83.63	ND	85.77	86.25	ND
25325/6	**67.1-70.1**	**65.31**	**ND**	**66.57**	**90.37**	**ND**
25332/1	17.7-21	103.61	ND	ND	102.48	ND
25332/2	38.1-41.1	99.19	ND	104.78	ND	ND
25332/3	50.9-55.5	94.70	ND	ND	ND	ND
25332/4	**66.8-69.8**	**49.33**	**ND**	**84.12**	**73.57**	**ND**
25327/1	18.9-21.9	123.36	101.31 (s)	ND	103.43	102.74
25327/2	57.9-60.9	84.16	93.78 (s)	ND	92.05	90.56
25327/3	**80.8-83.8**	**8.48**	**8.63 (s)**	**ND**	**25.79**	**56.08**
30092/1	17.7-20.7	ND	90.51 (w)	ND	ND	ND
30092/2	**48.2-49.4**	**ND**	**80.06 (w)**	**72.31**	**ND**	**66.92**
30092/4	108.2-110	ND	0.19 (w)	0.24	0.3	0.21

6 Conclusion

We have used multiple geochemical tracers to show that artesian discharge to a shallow alluvial aquifer is higher than previously derived from water balance models in the literature (Merrick 2000; CSIRO 2007; Kelly et al. 2007). This finding is important when considering the sustainable use of connected alluvial and artesian systems. We have also provided a percentage estimate of GAB groundwater in each sample collected in the LNA using the concentration of Cl in the groundwater, showing that in some locations the 'alluvial' sample is comprised of up to 70% GAB groundwater.

Isotopic tracers (^{3}H, ^{14}C, and ^{36}Cl) indicate that there is substantial mixing between two groundwater end-members of very different residence times (< 70 a and ~ 900 ka). This suggests interaction between modern surface recharge through the shallow LNA and variable artesian inflow at depth, dependent on where the sample is located in the system. Using past ^{14}C data (1978, 2003, 2010), along with data from this study to show that there has been an increase in ^{14}C in the groundwater in some locations of the LNA in the last ~ 40 years. This

suggests a greater contribution from modern river and flood recharge in locations proximal to the Namoi River since 1978, which could be induced by nearby groundwater abstraction for irrigation. In contrast, a sample farther from the river has displayed a steady decrease in ^{14}C content since 1978. How these trends change geographically throughout the system, and how they will behave in the future are difficult to constrain without continuous monitoring.

Recharge inputs to the LNA from the GAB were previously considered less than 22% (Merrick 2000; CSIRO 2007; Kelly et al. 2007). However, the geochemical data reported above clearly indicate that GAB discharge is occurring in locations where inflow is not apparent from the nested hydrograph data. This highlights the need to apply multiple groundwater investigation techniques (including flow modelling, hydrograph analysis, geophysics, and geochemistry) when inferring artesian discharge to an alluvial aquifer. This research has demonstrated that a multi-tracer geochemical approach is required to better determine artesian contributions to the alluvial aquifer and must be considered in constraining future models of the study system and elsewhere.

Acknowledgements

This research was funded by the Cotton Research and Development Corporation (CRDC). Charlotte Iverach was supported by scholarships from the Australian Government, ANSTO and CRDC. ANSTO support and analytical staff are thanked for their continuous efforts (Chris Dimovski, Henri Wong, Robert Chisari, Vladimir Levchenko, Krista Simon, Alan Williams, Simon Varley). The authors also thank Dr. Lisa Williams for editing and proofreading the manuscript. In addition, many thanks to the three reviewers, who provided constructive feedback and raised the overall quality of the paper.

Author contributions

Experimental conceptualisation and design was carried out by D.I.C & B.F.J.K. Fieldwork was conducted by C.P.I., D.I.C., S.I.H. & B.F.J.K. Additional data was contributed by K.T.M. Geochemical analyses were conducted by C.P.I., D.I.C. & K.M.W. The manuscript was written by C.P.I with input from all authors.

Competing Interests

The authors declare that they have no conflict of interest.

6 References

Abid, K., Dulinski, M., Ammar, F.H., Rozanski, K. & Zouari, K. Deciphering interaction of regional aquifers in Southern Tunisia using hydrochemistry and isotopic tools. *Appl. Geochem.* **27**, 44-55, 2012.

Acworth, R.I., Timms, W.A., Kelly, B.F.J., McGeeney, D.E., Ralph, T.J., Larkin, Z.T. & Rau, G.C. Late Cenozoic paleovalley fill sequence from the Southern Liverpool Plains, New South Wales – implications for groundwater resource evaluation. *Aus. J. Earth. Sci.* **62(6)**, 657-680, (2015).

Airey, P.L., Calf, G.E., Campbell, B.L., Habermehl, M.A., Hartley, P.E., & Roman, D., 1979. Aspects of the isotope hydrology of the Great Artesian Basin, Australia. In: Isotope Hydrology 1978, 1, P. 205–219. Proceedings International Symposium on Isotope Hydrology - International Atomic Energy Agency and United Nations Educational, Scientific and Cultural Organisation, Neuherberg, Fed. Rep. Germany, 19–23 June 1978. International Atomic Energy Agency, Vienna, 1979.

Amiri, V., Nakhaei, M., Lak, R. & Kholghi, M. Geophysical, isotopic, and hydrogeochemical tools to identify potential impacts on coastal groundwater resources from Urmia hypersaline Lake, NW Iran. *Environ. Sci. Poll. Res.* **23(16)**, 16738-16760, 2016.

Anderson, M.P. & Woessner, W.W. Applied Groundwater Modelling: Simulation of Flow and Advective Transport. Academic Press. ISBN: 0-12-059485-4, 1992.

Andrews, J. N. & J.-C. Fontes, Comment on chlorine 36 dating of very old groundwater, 3, Further results on the Great Artesian Basin, Australia by T. Torgersen et al., *Water Resour. Res*., **296**, 1871–1874, 1993.

Barnett B, Townley LR, Post V, Evans RE, Hunt RJ, Peeters L, Richardson S, Werner AD, Knapton A and Boronkay A. Australian groundwater modelling guidelines, Waterlines report, National Water Commission, Canberra, 2012.

Barrett, C. Upper Namoi groundwater source – status report 2011. NSW Department of Primary Industries, Office of Water, Sydney, 2012.

Bentley, H.W., Phillips, F.M., Davis, S.N., Habermehl, M.A., Airey, P.L., Calf, G.E., Elmore, D., Gove, H.E. Torgersen, T. Chlorine 36 dating of very old groundwater. 1. The Great Artesian Basin, Australia. *Water Resour. Res.* **22(13)**, 1986.

Beven, K. Environmental Modelling: An Uncertain Future? Routledge, ISBN-13: 978-0415457590 ISBN-10: 0415457599, 2009.

Calf, G.E. An investigation of recharge to the Namoi Valley aquifers using environmental isotopes. *Aust. J. Soil Res.* **16**, 197-207, 1978.

Cartwright, I., Weaver, T., Cendón, D.I. & Swane, I. Environmental isotopes as indicators of inter-aquifer mixing, Wimmera region, Murray Basin, Southeast Australia. *Chem. Geol.* **277**, 214-226, 2010.

Cartwright, I., Fifield, L.K. & Morgenstern, U. Using ^{3}H and ^{14}C to constrain the degree of closed-system dissolution of calcite in groundwater. *Appl. Geochem.* **32**, 118-128, 2013.

Cendón, D.I., Larsen, J.R., Jones, B.G., Nanson, G.C., Rickleman, D., Hankin, S.I., Pyeyo, J.J. & Maroulis, J. Freshwater recharge into a shallow saline groundwater system, Cooper Creek floodplain, Queensland, Australia. *J. Hydrol.* **392 (3-4)**, 150-163, 2010.

Cendón, D.I., Hankin, S.I., Williams, J.P., Van der ley, M., Peterson, M., Hughes, C.E., Meredith, K., Graham, I.T., Hollins, S.E., Levchenko, V. & Chisan, R. Groundwater residence time in a dissected and weathered sandstone plateau: Kulnura-Mangrove Mountain aquifer, NSW, Australia. *Aus. J. Earth Sci.* **61(3)**, 475-499, 2014.

Chen, Z., Nie, Z., Zhang, G., Wan, L. & Shen, J. Environmental isotopic study on the recharge and residence time of groundwater in the Heihe River Basin, northwestern China. *Hydrogeol. J.* **14(8)**, 1635-1651, 2006.

Clark, I.D. & Fritz, P. Age Dating Old Groundwater *in* Environmental Isotopes in Hydrogeology. CRC Press, USA, 1997.

Costelloe, J.F., Irvine, E.C., Weestern, A.W. & Tyler, M. Identifying fluvial recharge and artesian upwards leakage contributions to arid zone shallow, unconfined groundwater. *Chem. Geol.* **326-327**, 189-200, 2012.

CSIRO. Water availability in the Namoi. A report to the Australian Government from the CSIRO Murray-Darling Basin Sustainable Yields Project. CSIRO, Australia. 154pp., 2007.

763
764 Currell, M.J., Werner, A.D., McGrath, C., Webb, J.A. & Berkman, M. Problems with the application of
765 hydrogeological science to regulation of Australian mining projects: Carmichael Mine and Doongmabulla
766 Springs. *J. Hydrol.* **548**, 674-682, 2017.
767
768 Dawes, W.R., Gilfedder, M., Walker, G.R. & Evans, W.R. Biophysical modelling of catchment-scale surface
769 water and groundwater response to land-use change. *Math. Comp. Sim.* **64 (1)**, 3-12, 2004.
770
771 Department of Primary Industries (DPI) Water. NSW Government. *Namoi Alluvium Water Resource Plan*
772 *(GW14), Status and Issues Paper*, available at:
773 http://www.water.nsw.gov.au/__data/assets/pdf_file/0020/701732/Status-and-Issues-Paper-Namoi-GW-
774 WRP.pdf, 2017.
775
776 Duvert, C., Stewart, M.K., Cendón, D.I. and Raiber, M. Time series of tritium, stable isotopes and chloride
777 reveal short-term variations in groundwater contribution to a stream. *Hydrol. Earth Syst. Sci*. **20**, 257-277, 2016.
778
779 Fink, D., Hotchkis, M., Hua, Q., Jacobsen, G., Smith, A.M., Zoppi, U., Child, D., Mifsud, C., van der Gaast, H.,
780 Williams, A. & Williams, M. The ANTARES AMS facility at ANSTO. *Nuc. Instr. Meth. Phys. Res. Sect. B:*
781 *Beam Interac. Mat. Atoms* **223-224**, 109-115, 2004.
782
783 Gardner, W.P., Harrington, G.A. & Smerdon, B.D. Using excess ^{4}He to quantify variability in aquitard leakage.
784 *J. Hydrol.* **468-469**, 63-75, 2012.
785
786 Giambastiani, B.M.S., McCallum, A.M., Andersen, M.S., Kelly, B.F.J. & Acworth, R.I. Understanding
787 groundwater processes by representing aquifer heterogeneity in the Maules Creek Catchment, Namoi Valley
788 (New South Wales, Australia), *Hydrogeol. J.* **20(6)**, 1027-1044, 2012.
789
790 Golder Associates Santos Gunnedah Basin CSG Project. Groundwater impact study – Kahlua pilot test. Report
791 No. 107626100-005-Rev1. Golder Associates, Australia. 2010.
792
793 Herczeg, A.L., Torgersen, T., Chivas, A.R. & Havermehl, M.A. Geochemistry of ground waters from the Great
794 Artesian Basin, Australia. *J. Hydrol.* **126**, 225-245, 1991.
795
796 Hocking, M. & Kelly, B.F.J. Groundwater recharge and time lag measurement through Vertosols using impulse
797 response functions. *J. Hydrol.* **535**, 22-35, 2016.
798
799 Iverach, C.P., Cendón, D.I., Hankin, S.I., Lowry, D., Fisher, R.E., France, J.L., Baker, A. & Kelly, B.F.J.
800 Assessing connectivity between an overlying aquifer and a coals seam gas resource using methane isotopes,
801 dissolved organic carbon and tritium. *Sci. Rep*. **5**, 1-11, 2015.
802

Kalaitzis, P. & Jamieson, M. Draft Status Report for the Alluvial Groundwater Resources of the Lower Namoi Valley NSW. Land and Water Conservation Groundwater Unit Barwon Region, 121pp., 2000.

Kelly, B.F.J., Merrick, N., Dent, B., Milne-Home, W. & Yates, D. Groundwater Knowledge and Gaps in the Namoi Catchment Management Area. Cotton Catchment Communities CRC, University of Technology, Sydney – National Centre for Groundwater Management Report, NCGM 2007/1, 70pp., 2007.

Kelly, B.F.J., Timms, W.A., Andersen, M.S., McCallum, A.M., Blakers, R.S., Smith, R., Rau, G.C., Badenhop, A., Ludowici, K. & Acworth, R.I. Aquifer heterogeneity and response time: the challenge for groundwater management. *Crop & Past. Sci.* **64**, 1141-1154, 2013.

Kelly, B.F.J., Timms, W., Ralph, T.J., Giambastiani, B.M.S., Communian, A., McCallum, A.M., Andersen, M.S., Blakers, R.S., Acworth, R.I. & Baker, A. A reassessment of the Lower Namoi Catchment aquifer architecture and hydraulic connectivity with reference to climate drivers. *Aus. J. Earth Sci.* **61**, 501-511, 2014.

Lower Namoi Groundwater, NSW Government Department of Water and Energy, DWE_08_011, 2008, http://www.water.nsw.gov.au/__data/assets/pdf_file/0005/548699/wsp_namoi_gw_info_sheet.pdf

Love, A.J., Herczeg, A.L., Sampson, L., Cresswell, R.G., & Fifield, L.K. Sources of chloride and implications for 36Cl dating of old groundwater, southwestern Great Artesian Basin, Australia, *Water Resour. Res.* **36**, 1561-1574, 2000.

Mahara, Y., Habermehl, M.A., Miyakawa, K., Shimada, J. and Mizuochi, Y. Can the 4He clock be calibrated by 36Cl for groundwater dating? Nucl. Instr. Meth. in Phys. Res. Sect. B: Beam Interactions with Materials and Atoms **259**, 536-546, 2007.

Martin, H.A. Cenozoic climatic change and the development of the arid vegetation in Australia. *J. Arid Environ.* **66(3)**, 533-563, 2006.

Martinez, J.L., Raiber, M. & Cendón, D.I. Using 3D geological modelling and geochemical mixing models to characterise alluvial aquifer recharge sources in the upper Condamine River catchment, Queensland, Australia. *Sci. Tot. Environ.* **574**, 1-18, 2017.

Mawhinney, W. *Namoi Water Quality Project 2002-2007 – Final report*, NSW Office of Water, Sydney, 39 pp, 2011. Available at: http://pandora.nla.gov.au/pan/126486/20110413-1101/namoiwater.pdf

McLean, W.A. *Hydrogeochemical evolution and variability in a stressed alluvial aquifer system: Lower Namoi River catchment, NSW.* PhD thesis, University of New South Wales, Sydney (unpublished), 2003.

Meredith, K.T., Han, L.F., Hollins, S.E. Cendón, D.I., Jacobsen, G.E. & Baker, A. Evolution of chemical and isotopic composition of inorganic carbon in a complex semi-arid zone environment Consequences for groundwater dating using radiocarbon. *Geochim. et Cosmochim. Acta* **188**, 352-367, 2016.

Merrick, N.P. *Optimisation Techniques for Groundwater Management*. PhD Thesis, University of Technology, Sydney (unpublished), 551p.

Mook & van der Plicht. Reporting 14C activities and concentrations. *Radiocarbon* **41**, 227-239, 1999.

Moya, C.E., Raiber, M., Taulis, M. and Cox, M.E. Using environmental isotopes and dissolved methane concentrations to constrain hydrochemical processes and inter-aquifer mixing in the Galilee and Eromanga Basins, Great Artesian Basin, Australia. *J. Hydrol.* **539**, 304-318, 2016.

Nishiizumi, K. 10Be,26Al,36Cl, and 41Ca AMS standards: Abstract O16-1. In 9th Conference on Accelerator Mass Spectrometry, page 130, 2002.

NSW Pinneena Groundwater Database, NSW Government DPI Water, available at: http://allwaterdata.water.nsw.gov.au/water.stm, (last access: 19 May 2017), 2017.

Phillips, F.M. Chlorine-36, *in* Environmental Tracers in Subsurface Hydrology. Pp 299-348, 2000

Plummer & Glynn. Radiocarbon dating in groundwater systems. In: Isotope methods for dating old groundwater: — Vienna : International Atomic Energy Agency, 2013. Pp. 33-89, STI/PUB/1587, 2013.

Powell, J. & Scott, F. A representative irrigation farming system in the Lower Namoi Valley of NSW: an economic analysis. Economic Research Report No. 46, Industry and Investment NSW, 63pp., 2011.

Price, G. & Bellis, L. Namoi Catchment Water Study Independent Report Final Study Report. Schlumberger Water Services (Australia) Pty Ltd, 50371/P4-R2 FINAL, 129pp., 2012.

Puls, R.W. & Barcelona, M.J. Low-flow (minimal drawdown) groundwater sampling procedures. EPA/540/S-95/504, 10pp., 1996.

Radke, B.M., Ferguson, J., Cresswell, R.G., Ransley, T.R. & Habermehl, M.A. Hydrochemistry ad implied hydrodynamics of the Cadna-owie-Hooray Aquifer Great Artesian Basin. *Bureau of Rural Sciences, Canberra*, 2000.

Raiber, M., Webb, J.A., Cendón, D.I., White, P.A. & Jacobsen, G.E. Environmental isotopes meet 3D geological modelling: Conceptualising recharge and structurally-controlled aquifer connectivity in the basalt plains of south-western Victoria, Australia. *J. Hydrol.* **527**, 262-280, 2015.

Rawling, G.C. & Newton, B.T. Quantity and location of groundwater recharge in the Sacramento Mountains, south-central New Mexico (USA), and their relation to the adjacent Roswell Artesian Basin. *Hydrogeol. J.* **24(4)**, 757-786, 2016.

Reilly T.E. and Harbaugh A.W. Guidelines for Evaluating Ground-Water Flow Models, USGS Scientific Investigations Report 2004-5038, available at: https://pubs.usgs.gov/sir/2004/5038/PDF.htm, 2004.

Robertson, W.D. & Cherry, J.A. Tritium as an indicator of recharge and dispersion in a groundwater system in Central Ontario. *Water Resour. Res.* **25(6)**, 1097-1109, 1989.

"Drilling Methods Bring Spectacular Yield Increases." Rural Forum for Applied Research *in* North Western Courier [Narrabri] 11 Dec. 1967: 2. Print.

Salameh, E. & Tarawneh, A. Assessing the imapcts of uncontrolled artesian flows on the management of groundwater resources in the Jordan Valley. *Environ. Earth Sci.* **76**, 2017.

Scanlon, B.R., Healy, R.W. & Cook, P.G. Choosing appropriate techniques for quantifying groundwater recharge. *Hydrogeol. J.* **10 (1)**, 18-39, 2002.

Schilling, K.E., Jacobsen, P.J., Libra, R.D., Gannon, J.M., Langel, R.J. & Peate, D.W. Estimating groundwater age in the Cambrian-Ordovician aquifer in Iowa: implications for biofuel production and other water uses. *Environ. Earth Sci.* **76(2)**, 2016.

Sharma, P., Kuhik, P.W., Fehn, U., Gove, H.E., Nishiizumi, K. & Elmore, D. *Nucl. Instr. Meth. B.* **52**, 410-415, 1990.

Short, M.A., de Caritat, P. & McPhail, D.C. Continental-scale variation in chloride/bromide ratios of wet deposition. *Sci. Tot. Environ.* 574, 1533-1543, 2017.

Stone, J.O., Allan, G.L., Fifield, L.K., et al. Cosmogenic chlorine-36 from calcium spallation. *Geochim. et Cosmochim. Acta* **60**:679–692, 1996.

Smithson, A.*Lower Namoi Groundwater Source: Groundwater Management Area 001 Groundwater Status Report 2008*, NSW Department of Water and Energy, Sydney, 2009.

Tadros, N.Z. The Gunnedah Basin, New South Wales. Vol. 12. *Department of Mineral Resources, Coal and Petroleum Geology Branch*, 1993.

Torgersen, T., Habermehl, M.A., Phillips, F.M., Elmore, D., Kubik, P., Jones, G.B., Hemmick, T. & Gove, H.E. Chlorine 36 Dating of Very Old Groundwater: 3. Further studies in the Great Artesian Basin, Australia. *Water Resour. Res.* **27(12)**, 3201-3213, 1991.

Tosaki, Y., Tase, N., Massmann, G., Nagashima, Y., eki, R., Takahashi, T., Sasa, K., Sueki, K., Matsuhiro, T., Miura, T. & Bessho, K. Application of ^{36}Cl as a dating tool for modern groundwater. *Nuc. Instr. Methods in Phys. Res. Sect. B: Beam Interact. with Mat. and Atoms.* **259(1)**, 479-485, 2007.

Wilcken, K.M., Fink, D., Hotchkis, M.A.C., Garton, D., Button, D., Mann, M., Kitchen, R., Hauser, T. & O'Connor, A. Accelerator Mass Spectrometry on SIRIUS: New 6 MV spectrometer at ANSTO, *Nucl. Inst. & Meth. in Phys. Res. B* xxx, xxx-xxx http://dx.doi.org/10.1016/j.nimb.2017.01.003, 2017.

Williams, R.M., Merrick, N.P. & Ross, J.B. Natural and induced recharge in the Lower Namoi Valley, New South Wales *in* Sharma, M.L. (ed.) *Groundwater Recharge*, Proceedings of the Symposium on Groundwater Recharge, 239-253, 1989.

Zhang, L., Walker, G.R. & Dawes, W.R. Water balance modelling: concepts and applications. In. *Regional Water and Soil Assessment for Managing Sustainable Agriculture in China and Australia.* ACIAR Monograph No. 84, 31-47, 2002.

List of Figures

Figure 1. Map of the study area and sample locations, along with the location of the study area in Australia. Accompanying hydrographs show the groundwater level response in different piezometers throughout the study area (groundwater level data sourced from BOM 2017). The different colours in the hydrographs represent the different monitoring bores in the nested set. The bottom of the slotted interval for each bore is shown in the key. The x-axis in each hydrograph is the year (1970-2010) and the y-axis is depth (between 0 and 40 m below ground surface (bgs)). The two locations with red text highlight areas where the hydrograph heads show clear GAB contribution, with the deeper piezometer showing a higher head than the shallow one. The remaining locations show no apparent GAB contribution to the LNA based on the hydrograph data.

Figure 2. Two cross sections through the study area, showing the location and depth of the samples in the alluvium and their proximity to formations of the GAB. Contacts obtained

952 from gas wells Nyora-1, Culgoora-1 and Turrawan-2, coinciding with our cross sections, are
953 added. Their locations are displayed on the map. The chlorine-36 data interpolated using the
954 'natural neighbours' algorithm is shown in each cross section.

955 **Figure 3.** a) Na^+ vs HCO_3^- showing the mixing trend that the alluvial samples form between
956 the Namoi River and samples from the GAB (Radke et al. 2000; McLean 2003). The shaded
957 blue ellipse represents all river chemistry data available for the Namoi River and tributaries
958 (this work (n=4), McLean 2003 (n=4), Mawhinney 2011 (n=79)); b) Na^+ vs F^- and c) Cl^-/Br^-
959 vs Cl^-, highlighting the mixing trend between the surface recharge and the GAB that we
960 observe in other geochemical indicators. The red dotted line represents the Cl^-/Br^- ratio for
961 rainfall and the blue dotted line is the seawater ratio.

962 **Figure 4.** Water stable isotopes in the LNA, showing the two separate mechanisms of
963 recharge; surface water recharge plotting along an evaporation trend line and potential inflow
964 from the GAB clustered with regional samples from the GAB (McLean 2003).

965 **Figure 5.** Plot of depth vs ^3H, highlighting the ^3H activity throughout the vertical
966 groundwater profile.

967 **Figure 6.** ^3H (TU) vs ^{14}C (pmc). This shows the mixing between groundwater with detectable
968 ^3H activity (as indicated by the red band) and groundwater with very low ^{14}C content (as
969 indicated by the dotted blue line).

970 **Figure 7.** $^{36}Cl/Cl$ ($x10^{-15}$) vs ^{14}C (pmc). The colour gradient represents the mixing between
971 the two major sources: surface water recharge (blue = modern) and the GAB (brown = old).
972 The shaded yellow ellipse encompasses the two outliers where the geochemistry is being
973 influenced by proximity to the Napperby Formation. The shaded pink ellipse is sample
974 25327-3 located in the irrigation area.

975 **Figure 8.** a) ^{36}Cl vs Cl^- concentration. The ^{36}Cl production arrow represents in situ ^{36}Cl
976 production as a result of high U and Th in host rocks; b) $^{36}Cl/Cl$ ratio ($x10^{-15}$) vs Cl^-/Br^-. The

977 dotted blue line represents the Cl^-/Br^- ratio in seawater and the dotted red line represents the
978 expected Cl^-/Br^- ratio for rainfall at Narrabri based on distance from the coast (Short et al.
979 2017).
980 **Figure 9.** Approximate percentages of GAB contribution to the LNA, calculated from
981 multiple geochemical tracers and major ion data.
982